Received: 24 September 2018 | Revised: 23 May 2019 | Accepted: 28 May 2019
DOI: 10.1111/fwb.13359

ORIGINAL ARTICLE

Freshwater Biology WILEY

A three-dimensional numerical model investigation of the impact of submerged macrophytes on flow dynamics in a large fluvial lake

Maxim Bulat[1,2] | Pascale M. Biron[1,2] | Jay R. W. Lacey[2,3] | Morgan Botrel[2,4] | Christiane Hudon[2,5] | Roxane Maranger[2,4]

[1]Department of Geography, Planning and Environment, Concordia University, Montréal, Québec, Canada

[2]Groupe de Recherche Interuniversitaire en Limnologie (GRIL), Montréal, Québec, Canada

[3]Département de Génie Civil, Université de Sherbrooke, Sherbrooke, Québec, Canada

[4]Département des Sciences Biologiques, Université de Montréal, Montréal, Québec, Canada

[5]Environment and Climate Change Canada, Montréal, Québec, Canada

Correspondence
Maxim Bulat, Department of Geography, Planning and Environment, Concordia University, 1455 De Maisonneuve Blvd. W., Montréal, QC H3G 1M8, Canada.
Email: contact@maximbulat.com

Funding information
Fonds de Recherche du Québec - Nature et Technologies (FRQNT) Strategic Initiatives for Innovation; Canadian Network for Research and Innovation in Machining Technology; Fonds de Recherche du Québec - Nature et Technologies (FRQNT) Scholarship; Natural Sciences and Engineering Research Council of Canada (NSERC) Discovery Grant; Natural Sciences and Engineering Research Council of Canada (NSERC) Scholarship

Abstract

1. Aquatic plants (macrophytes) are known to affect flow dynamics, contributing to flow resistance. Most studies on flow-vegetation interactions are performed in laboratory flumes and focus on the flow field around plants, with little research at the level of vegetation patches in large aquatic ecosystems. In most hydrodynamic models, increased drag due to plants is modelled by increasing the Manning's n roughness coefficient.
2. The objectives of this study were to: (1) develop a three-dimensional hydrodynamic model (Delft3D) applicable to large water bodies including a novel approach to represent macrophyte resistance (modified k-ε turbulence closure model); and (2) compare the modelled flow with field measurements for different vegetation configurations and patch arrangements. Work was carried out in Lake Saint-Pierre, a large fluvial lake of the St Lawrence River in Québec, Canada.
3. Results showed a marked increase in residence time in the zone affected by macrophytes when using the modified k-ε turbulence closure model compared to the Manning's n approach, particularly near the bed. An improved agreement with field measured depth-averaged velocity is obtained with this novel approach (correlation coefficient of 0.80 compared to 0.46 with Manning's n only). In addition, a good fit was obtained between vertical velocity profiles modelled and measured in the macrophyte zone. Sensitivity analysis revealed that the additional drag due to plants was closely associated with plant height, but that plant density played only a minor role in retarding velocities.
4. These findings indicate that it is possible to accurately quantify both the horizontal and vertical flow modulations resulting from submerged vegetation in large fluvial systems. Considering that the Delft3D model is capable of approximating measured velocity magnitude, preserving the logarithmic shape throughout the water column and reaching near-zero velocities without increasing the roughness coefficient, we recommend this modelling approach for future research on the impact of macrophytes on flow at the scale of vegetation patches in large water bodies comparable to Lake Saint-Pierre.

KEYWORDS
ecological services, hydrodynamics, Lake Saint-Pierre, modelling, residence time

1 | INTRODUCTION

Submerged aquatic vegetation (SAV) is a vital component of aquatic ecosystem and provides many critical ecosystem services (Carpenter & Lodge, 1986; Jeppesen, Sondergaard, Sondergaard, & Christofferson, 1997). Indeed, macrophyte patches create spawning and rearing habitats and serve as a source of diversified food for fish populations (Thomaz, Dibble, Evangelista, Higuti, & Bini, 2008), wintering waterbirds (Schmieder, Werner, & Bauer, 2006), and also provide protection from predators (Grenouillet, Pont, & Olivier, 2001; Katayama, 2014). The presence of macrophytes fosters aquatic invertebrates and zooplankton richness and biomass (Bolduc, Bertolo, & Pinel-Alloul, 2016; Rennie & Jackson, 2005). Submerged aquatic vegetation, however, may also markedly reduce water velocities (Boudreau, Leclerc, & Fortin, 1994; Marjoribanks, Hardy, Lane, & Parsons, 2014; Marjoribanks, Hardy, Lane, & Tancock, 2017; Morin, Leclerc, Secretan, & Boudreau, 2000; Morin et al., 2003), which in turn can influence major biogeochemical cycles (Bal et al., 2013). By facilitating sedimentation and increasing water residence time, SAV can enhance nutrient/metal processing and removal (e.g. Costa, Tavares, Martinez, Colares, & Martins, 2018; Madsen, Chambers, James, Koch, & Westlake, 2001; Maine, Sune, Hadad, Sánchez, & Bonetto, 2006). Quantifying the impact of macrophytes on flow dynamics is thus essential to estimate elemental fluxes and model nutrient budgets in rivers and lakes (Billen, Garnier, Ficht, & Cun, 2001; Garnier, Némery, Billen, & Théry, 2005; Hudon & Carignan, 2008; Janse, 1997; Justić, Rabalais, & Turner, 2002; Tall, Caraco, & Maranger, 2011).

In situ studies estimating the impact of vegetation on flow dynamics in aquatic ecosystems are rare, particularly at larger spatial scales. Indeed, most laboratory studies have used a simplified representation of plants using various types of materials to assess their potential impact on hydrodynamics (Fischer-Antze, Stoesser, Bates, & Olsen, 2001; Kubrak, Kubrak, & Rowinski, 2008; Murphy, Ghisalberti, & Nepf, 2007; Sharpe & James, 2006). The use of rigid cylinders to simulate plants is very common, with only a few studies representing plants as flexible strips (Dijkstra & Uittenbogaard, 2010; Kubrak et al., 2008) or as a complex three-dimensional (3D) point cloud (Boothroyd, Hardy, Warburton, & Marjoribanks, 2017). Some laboratory experiments have attempted to replicate the natural complexity of macrophytes by emulating different patterns (linear, random, staggered arrays of cylinders) (Kubrak et al., 2008; Murphy et al., 2007; Yang, 2008). Nevertheless, these laboratory experiments remain simplistic as the patterns and materials used bear little correspondence with natural settings (Vargas-Luna, Crosato, & Uijttewaal, 2015). Although drag on live plants has been examined in the laboratory (Sand-Jensen, 2003, 2008; Siniscalchi & Nikora, 2013; Statzner, Lamouroux, Nikora, & Sagnes, 2006), few studies have focused on real vegetation in natural settings, particularly at larger reach scale. For small streams, Nikora et al. (2008) found, by comparing multiple vegetation parameters across study sites, that the best roughness descriptors while assessing the effects of SAV on hydraulic resistance were probably the ratios of average canopy/plant height to average flow depth. Their study highlights that the effect of SAV on flow could be assessed using site-averaged parameters. One such parameter is the blockage factor where flow resistance is a function of plant patches formed by multiple stems and leaves (Green, 2005). The obstruction to flow created by vegetation results in large velocity variations inside and outside of the patch (Kleeberg, Köhler, Sukhodolova, & Sukhodolov, 2010). The additional drag is represented in this case either through cross-sectional or volumetric versions of the blockage factor.

Quantifying the hydrodynamic impacts of macrophytes for large rivers or estuaries remains a challenge. The main difficulty lies in the need for an adequate representation of the added drag caused by vegetation through an apparent drag coefficient, C_D (Vargas-Luna et al., 2015). In turn, the apparent drag coefficient and flow resistance have been shown to vary markedly with physical plant features or traits such as differences in stem width and length, structural plant rigidity or flexibility, plant posture (Boothroyd et al., 2017), and the amount of foliage (Vargas-Luna et al., 2015). Differences in experimental techniques, study design, and measurement methods/equipment account for the wide range of C_D reported in the literature (Statzner et al., 2006). Values of C_D for plants have been estimated as a function of: (1) velocity (O'Hare, Hutchinson, & Clarke, 2007; Sand-Jensen, 2003; Wunder, Lehmann, & Nestmann, 2011); (2) Reynolds number (based on submerged depth of vegetation and average velocity) (Wu, Shen, & Chou, 1999; Wilson, 2007); or (3) through other dimensions pertinent to aquatic vegetation, such as stem thickness or diameter. Stem thickness and diameter have also been used in combination with either average flow through vegetation (Cheng & Nguyen, 2011; Kothyari, Hashimoto, & Hayashi, 2009; Tanino & Nepf, 2008) or average velocity (Armanini, Righetti, & Grisenti, 2005; Wilson & Horritt, 2002). There is, however, insufficient attention paid to the influence of SAV on flow at the patch scale directly within aquatic ecosystems as existent models for drag/resistance are built on small-scale physically based empirical relationships using roughness parameters (e.g. C_D and/or Manning's n) and do not reflect the spatial variation within the flow field (Ayoub et al., 2018; Marjoribanks et al., 2017).

Another limitation in quantifying hydrodynamic impacts of SAV in numerical models at larger scales is that a numerical grid of high resolution is required to represent individual plants. Higher-resolution numerical grids increase calculation time substantially and require powerful computers or clusters to deal with multiple equations per time step. Brito, Fernandes, and Leal (2016) and Boothroyd et al.

(2017) argue that, for small scale study sites (4–20 m^2), SAV could be represented as porous media, thus eliminating the need of a high-resolution grid. However, it remains doubtful that such an approach is applicable at larger scales.

Several two-dimensional (2D) numerical models that include the impact of macrophytes for large waterbodies exist; for example, Morin, Leclerc, et al. (2000) and Li and Millar (2011) have represented the increased SAV in their models through elevated Manning's *n* values. Because most submerged plants are flexible and have different growth forms where many do not occupy the entire water column, a 3D hydrodynamic approach may better represent their true impact on the flow field. Moreover, while the effect of macrophytes on the shape of vertical velocity profiles has been previously examined in a laboratory setting (Aberle & Järvelä, 2013; Fischer-Antze et al., 2001; Hu, Huai, & Han, 2013; Nikora et al., 2013), to the best of our knowledge, no previous work has attempted to use a 3D numerical model to characterise velocity profiles at a large-scale field site. The objectives of our study are to: (1) develop a 3D hydrodynamic model (Delft3D; D3D) applicable to a large-scale field site (Lake Saint-Pierre [LSP], QC, Canada) including a novel approach to represent macrophyte resistance (modified 3D k-ε turbulence closure model); and (2) compare the modelled flow field with field measurements for different vegetation configurations and patch arrangements.

2 | METHODS

2.1 | Study area

Lake Saint-Pierre, a freshwater widening of the St Lawrence River (SLR) in Quebec, Canada (Figure 1), is a critical area for wildlife and aquatic species (Hudon & Carignan, 2008) with significant macrophyte coverage during the summer (Vis, Cattaneo, & Hudon, 2008). The surface of LSP covers about 300 km^2 and stretches for nearly 30 km in length (streamwise direction). The lake was chosen as a Ramsar site in 1998 (Ramsar Sites Information Service n.d.) (https://rsis.ramsar.org/ris/949), and in 2000 it was designated as UNESCO Biosphere Reserve (Canadian Commission for UNESCO, 2017). Several agricultural watersheds drain into LSP, mainly from the south shore (e.g. Yamaska, Saint-François, and Richelieu Rivers) (Goyette et al., 2016) and since it is located downstream from the greater Montreal area, it is also affected by urban wastewater pollution (Blaise, Gagné, Eullaffroy, & Férard, 2008; Marcogliese et al., 2015).

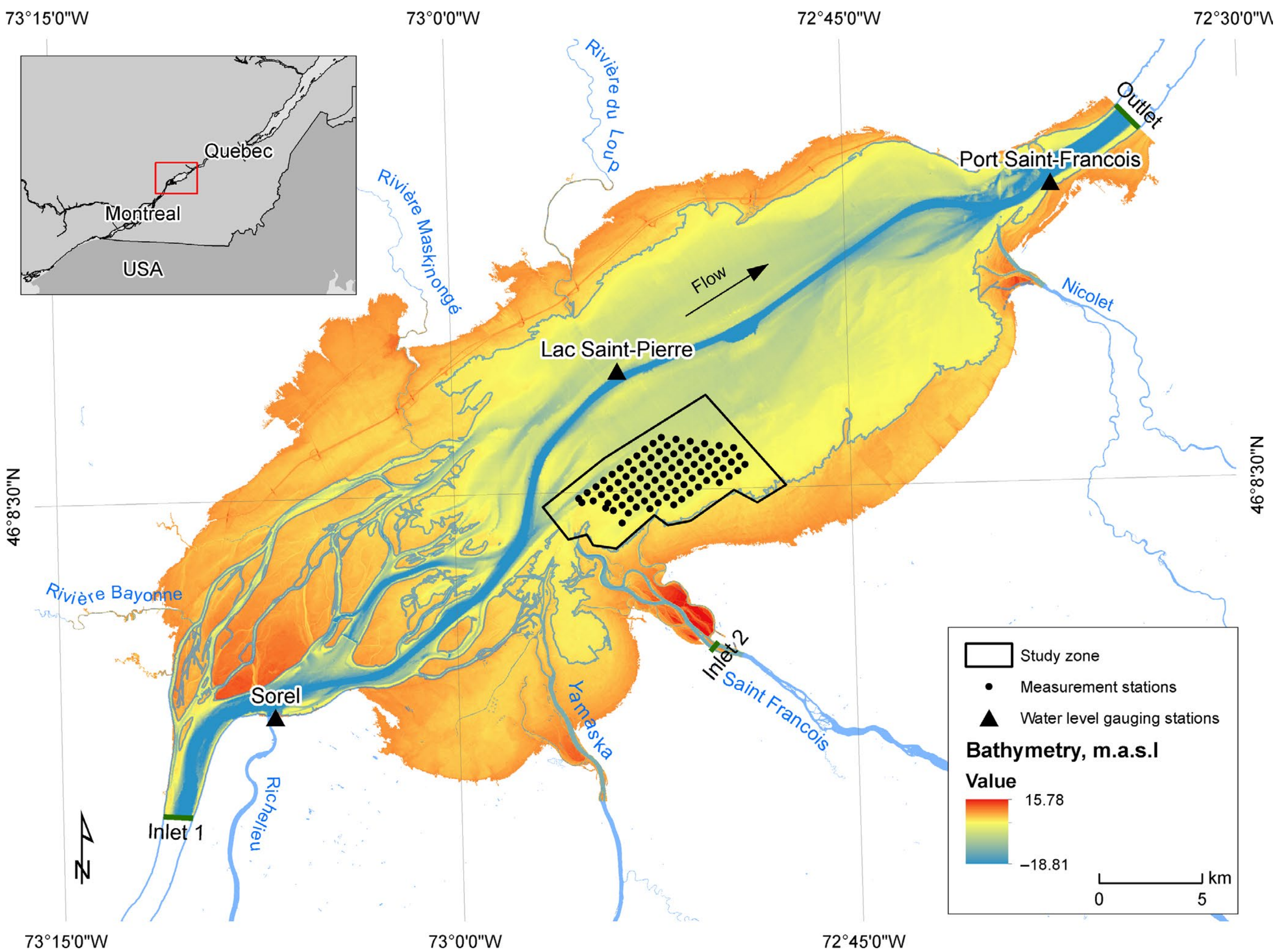

FIGURE 1 Location and bathymetry of Lake Saint-Pierre including the study zone at the mouth of the Saint-François River. Lake Saint-Pierre is located approximately 100 km north-east of Montreal (Quebec) [Colour figure can be viewed at wileyonlinelibrary.com]

TABLE 1 Mean daily discharge calculated for field data campaign dates for the St Lawrence River (SLR) at Sorel and the Saint-François River (SFR) at its confluence with Lake Saint-Pierre used in runs

Survey year	SLR discharge at Sorel (m^3/s)	SFR discharge (m^3/s)
2012	7,450	40.6
2013	9,015	107.5
2014	9,955	94.5
2015	9,898	135.2
2017	11,305	71.5

Most of the lake is relatively shallow, with an average depth of 3–4 m (Figure 1). A significant portion of the discharge is concentrated in the man-made central navigation channel, with depths exceeding 11 m (Hudon & Carignan, 2008). During July/August, approximately 85% of the LSP bed area is covered by submerged aquatic plants (Hudon & Carignan, 2008; Vis et al., 2008).

Starting in 2012 the strategic research cluster GRIL (Groupe de recherche interuniversitaire en limnologie) initiated a macrophyte and ecosystem service monitoring program of a *c*. 42 km^2 area of LSP downstream from the mouth of the Saint-François River (SFR; Figure 1). The established zone was selected due to characteristic extensive plant colonisation with high spatial variability in abundance (Vis et al., 2008; Hudon et al., 2012; de la Chenelière, Brodeur, & Mingelbier, 2014). The study zone includes approximately 60 measurement stations (Figure 1) that were surveyed at maximum macrophyte abundance (end of July, beginning of August) for a 6-year period (2012 to 2017).

Currently, a 2D hydrodynamic model of the SLR is used by Environment and Climate Change Canada (ECCC), which includes LSP (Martin, Champoux, & Morin, 2016; Morin, Leclerc, et al. 2000). This model characterises flow resistance due to SAV through a friction coefficient (Manning's *n*) (Boudreau et al., 1994; Talbot, 2006). Although this approach models reduced velocities in macrophyte zones, it does not represent near-zero velocity zones well, which are observed in some parts of LSP.

2.2 | Field data

Field measurements included the spatial distribution of macrophyte height and biomass as well as velocity measurements. Macrophyte measurements were performed annually using echo-sounding techniques, as well as direct sampling using the rake method (Yin, Winkelman, & Langrehr, 2000). Acoustic surveys were conducted on 250-m spaced transects perpendicular to the lake shore using a downward-looking single beam BioSonics DTX system with a 6.6° angle and a working frequency of 430 kH (pulse length of 0.1 ms, ping rate 5 ping/s). Data were post-processed in Visual Habitat 1 (BioSonics) and averaged for cycles of 5 pings. Macrophytes were also collected by raking the lake bed over a distance of about 1 m (0.35 m^2) at each station. Macrophyte biomass was estimated from the mean of three replicate rake samples collected around the boat and reported as g dry mass/m^2. Velocity measurements were taken with a propeller current meter (Swoffer 2100, accuracy within 1%) at three (2012–2015) or four (2017) heights above the bed. In 2012–2015, points were taken at 20, 40, and 80% of flow depth, and in 2017, an additional measurement was taken at 60% of the depth above the bed. Since only 2017 measurements included four depth points, for consistency purposes the observed depth-averaged velocity (DAV) was calculated with the two-point approach, taking the average values at 20% and 80% of the water depth (Julien, 1998).

Bed elevation data are particularly important for hydrodynamic model mesh generation. For our study, we used a digital elevation model (DEM) created in 2002 by ECCC. The DEM has a pixel resolution of 25 m and was created by combining LiDAR elevation and sonar bathymetry data. Measured historical water-level data were obtained from Fisheries and Oceans Canada for the following gauging stations: Sorel (#15930, upstream section), LSP (#15975, mid-lake location) and Port Saint-François (#3365, downstream section; Figure 1). The water level used in the model at the outlet boundary was linearly extrapolated using Sorel and Port Saint-François gauging stations. The estimated daily historical discharge data for the SLR at Sorel near the inlet (Figure 1) were provided by ECCC (Jean Morin, personal communication). The discharge data for the SFR were obtained from Hydro-Québec Chutes Hemming station (located 48 km upstream from the SFR mouth). A correction of 1.05, computed based on the ratio of drainage areas, was applied to estimate the discharge at the inlet of the SFR from the gauging station measurements (Inlet 2, Figure 1). The Yamaska, Richelieu, and other tributaries flowing into the lake were excluded from the model and considered insignificant (<10%) in comparison with the discharge of the SLR. Flow conditions varied between years, with 2012 representing the year with lowest discharge and flow stage for the SLR, and 2017 the highest (Table 1).

2.3 | Three-dimensional model: D3D

The model D3D, developed by Deltares, NL, was used in this study (version 4.01.01.rc.03, 11 August 2015). Delft3D is open-source software, that allows creating hydrodynamic models of fluvial, lacustrine, and coastal/tidal environments. It is based on the Navier–Stokes and continuity equations under the shallow water and the Boussinesq assumptions. The software can model flow dynamics in 2D and 3D and has the capacity to include sediment, nutrient, and pollutant transport. For 3D computation, vertical velocities are computed from the continuity equation.

2.3.1 | Selection of macrophyte modelling approach

The latest versions of D3D (since May 2014) include additional functionality to address the integration of drag due to the presence of bedforms (e.g. dunes) and macrophytes. Depending on the required type of modelling (2D or 3D), D3D offers application of two vegetation models: either trachytopes (from a Greek word meaning roughness), or a modified 3D k-ε turbulence closure model (Deltares, 2014). The modified 3D k-ε turbulence model (modified k-ε model) was successfully tested by Fischer-Antze et al. (2001) for laboratory conditions. Trachytope functionality defines resistance and bed roughness on a sub-grid scale (having several values per cell) through different resistance classes (referred to as trachytopes). In the modified k-ε model, aquatic plants are represented as rigid cylinders. The influence of the vegetation upon the momentum equations is given by the vertical distribution of the friction force as caused by cylindrical elements in oblique flow (Deltares, 2014). Effectively, to model the additional flow resistance of submerged vegetation, the drag force (F_D) on a rigid obstacle is introduced as a sink term into the Navier–Stokes equations (Fischer-Antze et al., 2001):

$$F_D = \rho/2\, U^2\, C_D\, \lambda$$

where ρ is the water density, U is the horizontal velocity and λ is a vegetative coefficient, which depends on the number of plants per unit area and stem width (Deltares, 2014).

Both functionalities (trachytope and modified k-ε model) were preliminarily tested in a simple flume model (Bulat, 2018) whose geometry was similar to the experimental setup described in Murphy et al. (2007) (their run H). The modelling results revealed negligible variation in velocities (<1% difference) using the trachytope function. Alternately, the modified k-ε model resulted in large velocity variations within the flow field, both vertically and horizontally. Near the bed, predicted velocities were 0.022 m/s, compared to 0.033 m/s in Murphy et al. (2007), whereas near the surface, they were nearly identical (0.11 m/s compared to 0.111 m/s in Murphy et al., 2007). The predicted mean velocity profiles also compared well with the flume measurements of Murphy et al. (2007). Based on these findings (reported in Bulat, 2018) it was decided to apply the modified k-ε model to the main LSP model.

2.3.2 | Model preparation

An initial model of LSP was built using the RGFGRID module in D3D. To simplify the model, only the confluence of the SLR with SFR was taken into account. The upstream boundary of the LSP (the Sorel–Berthier Archipelago) has a complex geometry, comprising of approximately 103 islands. Given this complexity, a Cartesian rectangular grid was preferred to a curvilinear one to avoid continuity problems during model computation. In total, the grid consisted of 796 × 260 cells out of which 140 133 (68%) were active elements. Five vertical layers were used. The average cell size was around 70 m. To focus on the area at the mouth of the SFR (study zone, Figure 1), a connected sub-grid was required. The grids were connected through domain decomposition where variables are transferred through the connecting boundaries. To determine the refinement factor of the sub-grid, a grid sensitivity analysis was conducted with three grid resolutions (of 76 × 55 m, 25 × 20 m, and 15 × 12 m) in the study zone (keeping a coarser fixed LSP grid size in all tests). Modelling results using the second grid refinement (factor of 3) revealed a percentage difference in maximum velocity from the finest resolution (refinement factor of 5) of <10%, which is considered a satisfactory threshold (Biron, Haltigin, Hardy, & Lapointe, 2007). The refinement factor of 3 was therefore used, resulting in average cell size in the study zone of approximately 25 m (Figure 2).

Delft3D allows utilisation of different roughness coefficients including Manning's n. Although the simplest approach was to use a single roughness coefficient value for the entire domain, we preferred the use of a generalised roughness coefficient map, to better represent the spatial variations in flow resistance, while considering the scale of LSP. Accordingly, the initial Manning's n value for the SLR (main navigational channel in the lake) and SFR in the model was set to 0.016, and the rest of the lake was assigned a value of 0.018

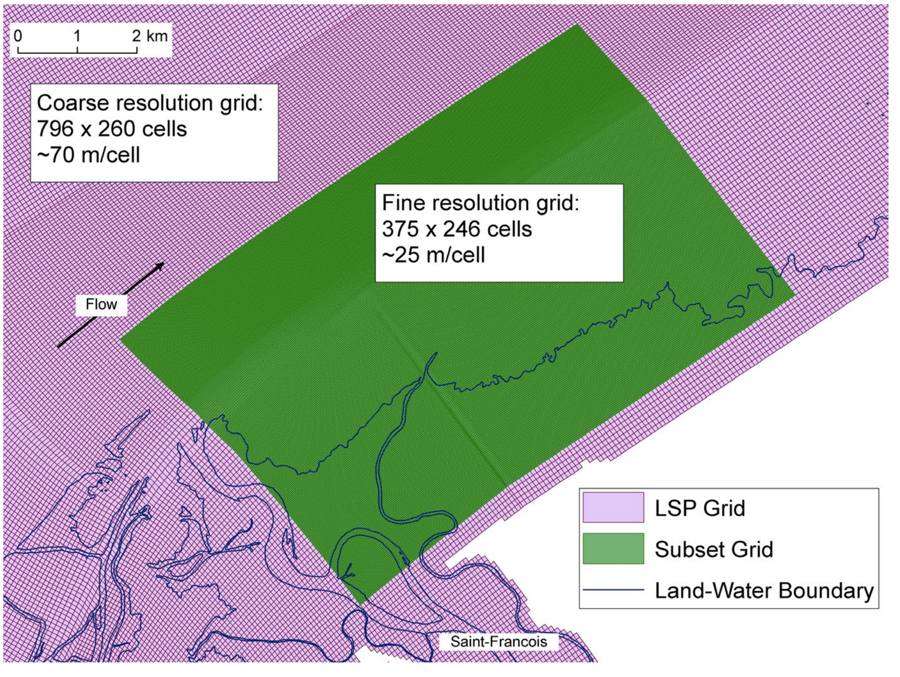

FIGURE 2 Spatial distribution of grids used in Lake Saint-Pierre (LSP) model, with a finer resolution in the study zone (in green) [Colour figure can be viewed at wileyonlinelibrary.com]

except for the study zone where n was equal to 0.038. These values were later modified at the calibration and validation stages.

Macrophytes in the study zone were represented via four scenarios:

1. Manning's *n* value;
2. Mannings's *n* and modified *k*-ε model applied assuming a homogeneous distribution of vegetation (0.75 m in height, single stem of 0.005-m diameter, and density of 500 rigid cylinders per m^2);
3. Mannings's *n* and modified *k*-ε model applied to large patches (based on the field observations of macrophyte coverage over 5 years [height of 0.75 m in height, 0.005-m diameter, 500 and 1000 cylinders/m^2 density]);
4. Mannings's *n* and modified *k*-ε model applied to small patches 100 × 100 m in area based on 2015 survey macrophyte data.

The background horizontal eddy viscosity was kept constant throughout all simulation runs at 0.0001 m^2/s, which is the recommended value for lakes in D3D (Deltares, 2014). The eddy viscosity term accounts for the added energy dissipation due to turbulence in the flow. A single average eddy viscosity value is sufficient for uniform flow; however, for complex geometries, distributed calibrated values of eddy viscosity are desirable (Papanicolaou, Elhakeem, & Wardman, 2010). The calibration of background horizontal eddy viscosity has been shown to play an important role in D3D model performance (Parsapour-Moghaddam & Rennie, 2018). However, such a calibration would have required very detailed velocity measurements throughout the numerical domain, which are difficult to obtain for large-scale studies such as LSP. Furthermore, a uniform eddy viscosity value was desired in order to clearly test the effect of the vegetation model on velocities. Sensitivity analyses were run for macrophyte heights and densities, starting with an average value for heights (0.35 m, based on field observations) and densities (500 cylinders/m^2, based on sensitivity analyses). These values were then progressively increased (0.65 and 1.00 m for heights, 750 and 1000 cylinders/m^2 for densities). For heights, a very high value of 1.35 m was also tested, even if in some cases this exceeded water depth, to better assess the impact of this variable on the numerical models.

2.4 | Model calibration and validation

The hydrodynamic model (without vegetation) was built and calibrated using 18 June 2012 discharge and water surface data. A low flow (19 August 2012) and high flow (2 October 2010) condition were used for model validation by comparing modelled and measured water levels at the three gauging stations. Table 2 summarises the boundary conditions used for calibration and validation. All models were run for 18 hr at steady-flow conditions and a 0.1-min time step.

TABLE 2 Boundary conditions used for calibration and validation

	2012/06/18	2012/08/19	2010/10/02
Discharge, Q_{SLR} (m^3/s)	7,990	7,198	12,400
Discharge, Q_{SFR} (m^3/s)	51	33	1,151
Water level$_{SLR}$ (*m*)	3.37	3.23	4.88

The calibration was performed by uniformly adjusting Manning's *n* values by small increments (0.0005) throughout the entire domain. The final values used in LSP model were n = 0.0235 for the main channel of the SLR (St Lawrence River) and the SFR (Saint-François River), n = 0.0455 for the study zone and n = 0.0255 for the rest of the lake. Validation results for low flow (19 August 2012) revealed an average difference in elevation of 1 cm, whereas for the higher flow conditions (10 October 2010), the average difference was 4 cm for the three water level stations (Table 3). The model thus appeared to adequately reproduce water levels of LSP under a wide range of flow conditions.

3 | RESULTS

3.1 | Macrophyte distribution and parameterisation

The macrophyte field data reveal high inter-annual variability in both the biomass and plant height, with higher values in 2013 and 2015 (Figure 3a,b). Consistent patterns of dense (30–150 g dry mass/m^2) and high (0.35–1.00 m) SAV were observed close to the confluence with the SFR and along the right downstream bank of LSP, where macrophytes occupied up to 70% of the total water column (i.e. flow depth). Based on an average pattern of biomass for the 5-year study period (Figure 3a), the large patches used in modelling scenario 3 were defined manually in a Geographical Information System with dense (1,000 plants/m^2) patches close to the right bank fringed by two smaller, more scattered (500 plants/m^2) vegetation patches located farther from the bank (large patches scenario; Figure 4).

TABLE 3 Validation results based on comparing water level at the gauging station locations

Date	Gauging station	Measured, m	Modelled, m	Difference, m
2012/08/19 (low flow)	Sorel	3.775	3.775	0
	Lake Saint-Pierre	3.427	3.444	0.02
	Port Saint-François	3.251	3.25	0.01
2010/10/02 (high flow)	Sorel	5.482	5.539	0.06
	Lake Saint-Pierre	5.127	5.163	0.04
	Port Saint-François	4.950	4.928	0.02

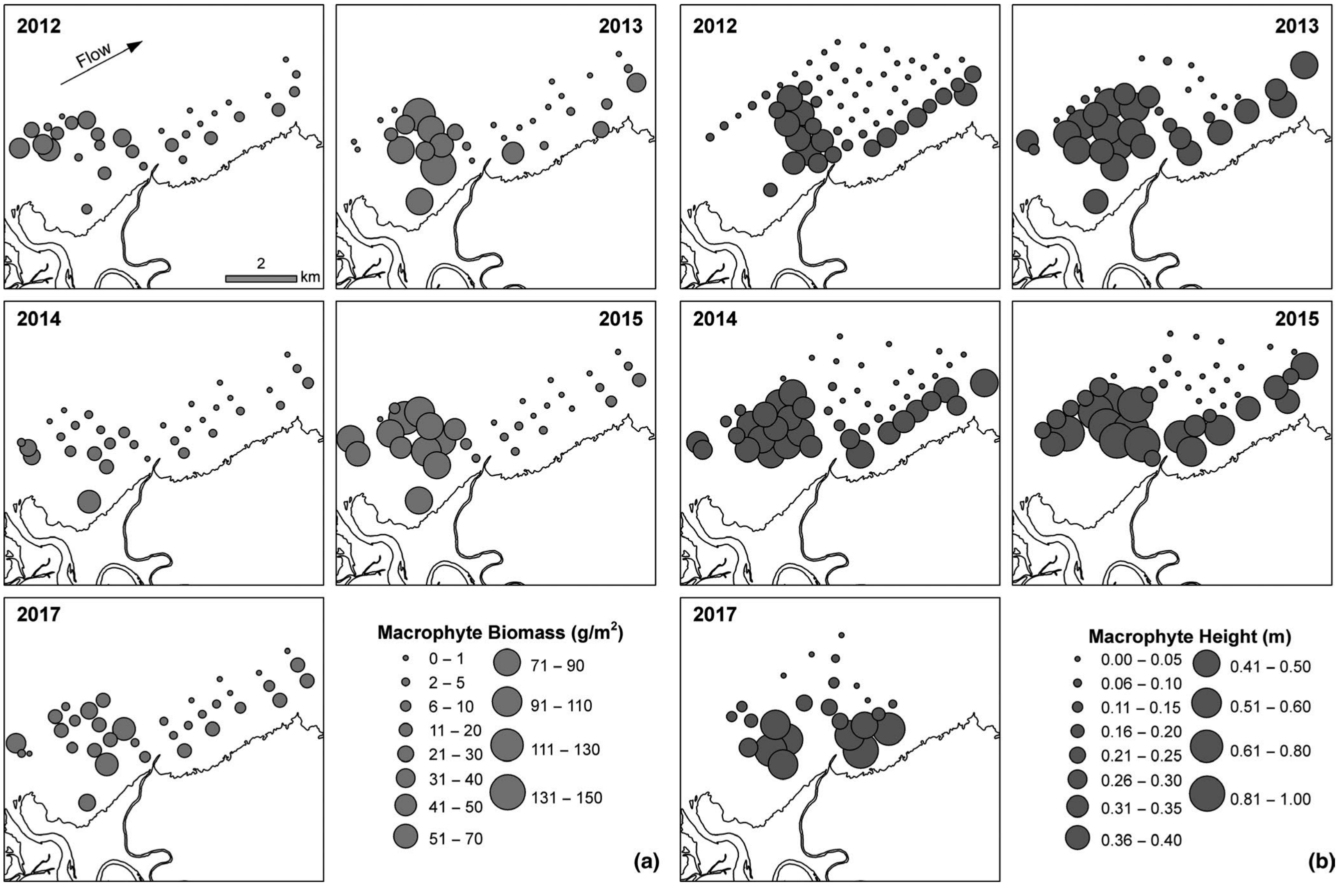

FIGURE 3 Spatial variation of total macrophyte biomass (g dry mass/m^2) collected (a) and macrophyte height (m) (b) at the measurement stations. Flow in Lake Saint-Pierre is from left to right (see arrow in upper left panel)

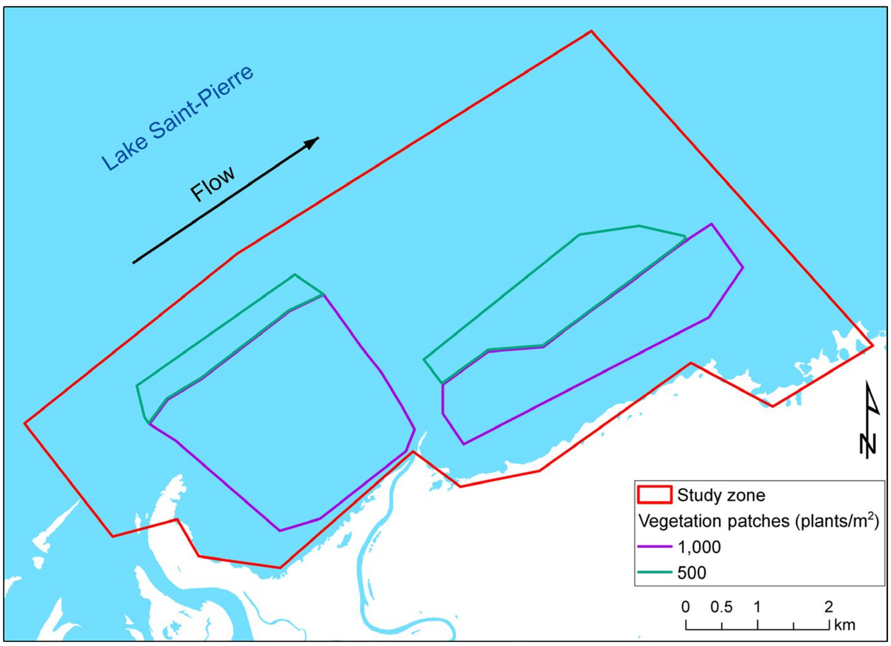

FIGURE 4 Location of the modelled patches inside the study zone with either 500 or 1,000 plants/m^2 (large patches scenario) [Colour figure can be viewed at wileyonlinelibrary.com]

3.2 | Spatial distribution of velocities

Measured velocity profiles in the study zone reached a maximum of V = 0.34–0.50 m/s near the water surface (80% depth from the bed). Depth-averaged velocities are presented in Figure 5 and ranged between 0.06 and 0.11 m/s. Overall faster flow was observed farther from the bank towards the navigational channel. The flow slowed in the mid-section of the zone and reached near-zero velocities near the shore. Comparisons between the plant biomass (Figure 3a) and DAVs (Figure 5) show that the elevated biomass at the mouth of the SFR coincided with markedly reduced velocities in the study zone (Figure 5).

3.3 | Numerical modelling—impacts of macrophytes on residence time

3.3.1 | Depth-averaged results

The spatial variability in modelled water velocity is best illustrated using the depth-averaged results. The August 2017 flow condition (Q = 11,377 m^3/s) is presented in Figure 6a and is representative of all the surveyed years. In Figure 6a, marked differences in velocity are observed between the main (navigation) channel of the SLR, peaking at 1.2 m/s, and the markedly slower flow along the banks, including the study zone, with velocity below 0.1 m/s. The model results presented in Figure 6a,b are based on using Manning's *n* to represent increased macrophyte roughness near the STF confluence. Overall, the modelled flow field corresponded well to field measurements (Figure 6b), but there are a few stations closer to the navigational channel where the velocity is underestimated (in white in Figure 6b) and, most importantly, the velocity of 42.6% of the stations, primarily near the bank, were overestimated by the model (black circles in Figure 6b). This highlights the limitations of a model solely based on Manning's *n* to predict very low velocities associated with macrophytes as the assumption of a logarithmic profile is unrealistic in a flow field affected by vegetation. Therefore, even with very high Manning's *n* values, the near-zero velocities would not be adequately simulated. Introducing additional drag due to macrophytes into the LSP model through the modified k-ε model (homogeneous distribution of vegetation) yielded a decrease in flow velocity with a better agreement (4.3% of the stations with overestimated velocity) with the field measurements near the right bank (Figure 6c).

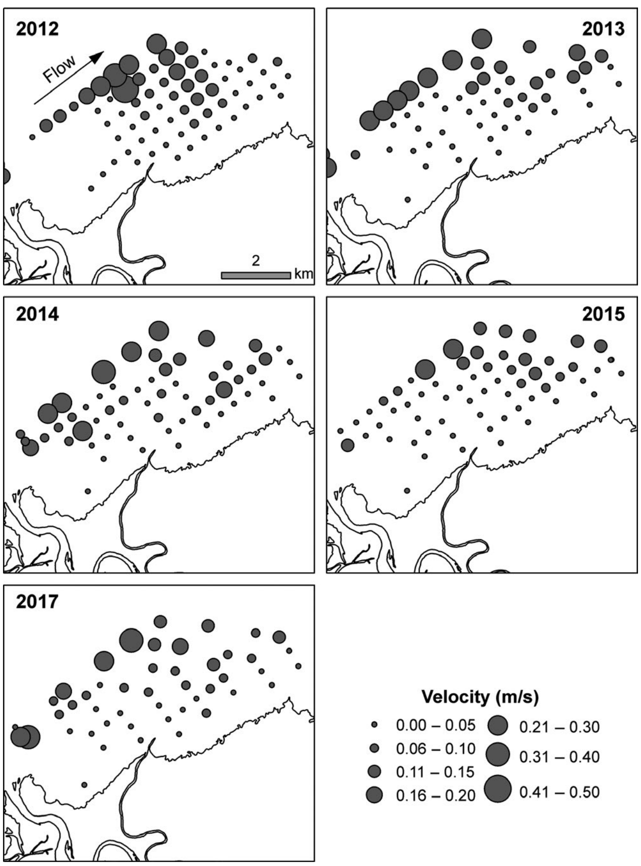

FIGURE 5 Field measurements of depth-averaged velocity (m/s) at measurement stations

The decrease in flow velocity resulting from the additional drag due to macrophytes through the modified k-ε model corresponds to an increase in water retention time in the study zone. This was tested for five different flow events from 2012 to 2017 by comparing the first scenario (Manning's *n* only) with the models incorporating Manning's *n* and additionally the modified k-ε model to represent macrophytes either as a homogeneous zone covering all sampling stations (0.75-m plant height and 500 plants/m^2 density) or as large patches (Figure 4).

The DAV for each scenario averaged for different flow events over the 5-year period reveals that the homogeneous distribution of macrophytes resulted in the largest increase of mean residence time in comparison with predictions modelled using Manning's *n*. The mean residence time was estimated by dividing the longitudinal distance of the study zone, 9.7 km, by the DAV. The homogeneous distribution is seen to increase the mean residence time by 6.2 hr (Table 4). The inclusion of large vegetation patches in the model (covering 15 km^2) is seen to exert a lesser impact on mean residence times than a homogeneous plant cover, which assumes SAV over the entire zone of 42 km^2. The patches nevertheless increased mean residence time by 3.2 hr.

3.3.2 | Vertical differences in the water column

In 2015, a high density of macrophytes was measured at the field site. This year was therefore used to compare velocities and mean residence time predicted by the Manning's *n* and homogeneous models at three different relative heights above the river bed (bottom (z/H = 0–0.2); middle (z/H = 0.4–0.6); surface layer (z/H = 0.8–1.0), where z is the height above the bed and H was the total depth at a specific location. Statistical analysis (*t*-test, α = 0.05) showed that the mean velocity modelled using the homogeneous macrophyte distribution and modified k-ε model were significantly reduced near the river bed and in the middle of the water column in comparison with the Manning's *n* only model (Figure 7, Table 5). Accordingly, mean residence times for the homogeneous scenario were increased by 5.8 hr in the middle layer and 22.8 hr in the bottom layer, assuming a parcel of fluid remains at the same elevation as it advects downstream. No significant difference in top-layer (near surface) mean velocity or residence time between values predicted using the Manning's *n* only model and that derived from the homogeneous macrophyte distribution with the modified k-ε model.

FIGURE 6 Modelled depth-averaged velocity for the August 2017 dataset: (a) whole domain using Manning's *n* only; (b) study zone using Manning's *n* only; and (c) study zone using Manning's *n* and the modified *k*-ε model. Velocity comparison between the predicted and measured velocity at measurement stations, showing where the model underestimates (white circles), overestimates (black circles), or approximates field observations (grey circles, within ± 0.05 m/s) [Colour figure can be viewed at wileyonlinelibrary.com]

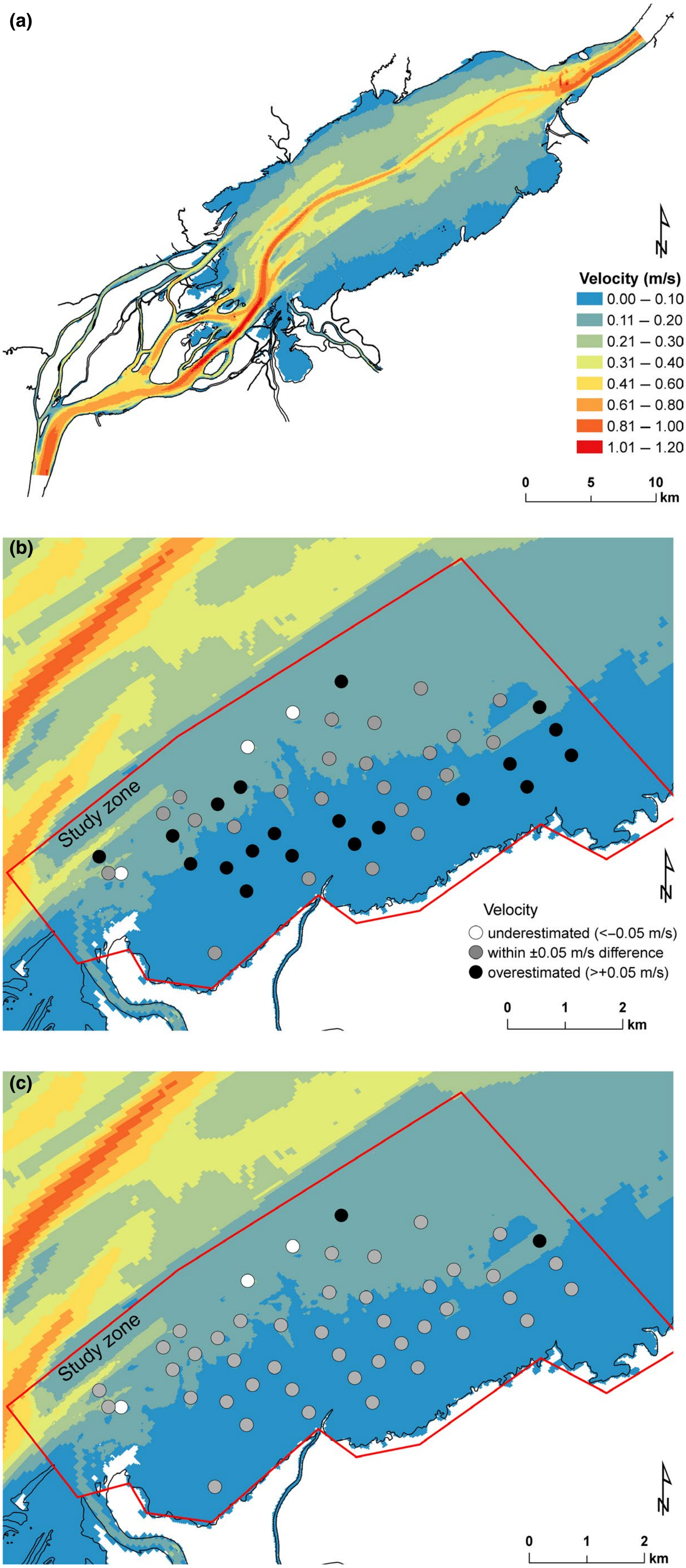

TABLE 4 Comparison of mean 2012–2017 water residence time based on the spatial mean depth-averaged velocity (DAV), for the three scenarios of macrophyte roughness modelled using the modified 3D *k*-ε turbulence model

Scenario	Mean DAV, m/s	Mean DAV standard deviation, m/s	Mean residence time, hr	Mean difference in residence time, hr
Manning's *n* only	0.120	0.0089	22.4	–
Small patches (*k*-ε model)	0.120	0.0700	22.4	–
Large patches (*k*-ε model)	0.105	0.0050	25.6	3.2
Homogeneous (*k*-ε model)	0.094	0.0089	28.6	6.2

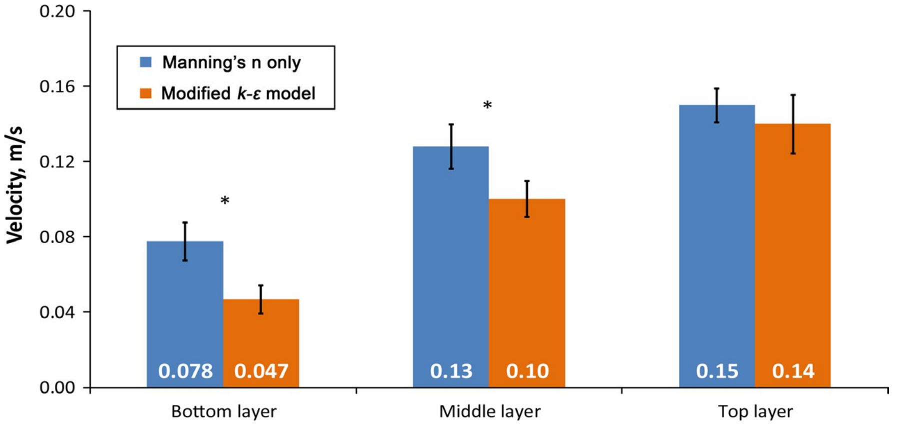

FIGURE 7 Comparison of mean velocity for the whole study zone derived from values modelled using Manning's *n* or homogeneous macrophyte distribution scenarios (with the modified *k*-ε model). Velocity values were modelled separately for the bottom layer near the river bed (z/H = 0–0.2), in the middle layer (z/H = 0.4–0.6), and in the surface (top) layer (z/H = 0.8–1.0) of the water column. Significant differences in velocity are indicated by the star symbol [Colour figure can be viewed at wileyonlinelibrary.com]

TABLE 5 Comparison of mean longitudinal velocity and mean water residence time between the Manning's *n* only and homogeneous submerged aquatic vegetation with modified *k*-ε modelling methods for 3 vertical water layers located at increasing height above the river bed

	Mean velocity, m/s		Standard deviation, m/s		Residence Time, hr		
Layer *z/H*	Manning's n only	Homogeneous, *k*-ε model	Manning's *n* only	Homogeneous, *k*-ε model	Manning's *n* only	Homogeneous, *k*-ε model	Difference, hr
Top (0.8–1.0)	0.15	0.14	0.08	0.01	17.9	19.2	1.3
Middle (0.4–0.6)	0.13	0.10	0.07	0.09	21.0	26.8	5.8
Bottom (0–0.2)	0.078	0.047	0.05	0.06	34.6	57.4	22.8

3.4 | Numerical modelling—comparison with field observations

3.4.1 | Entire study zone

As presented in Section 3.4.2, we tested the effect of smaller vegetation patches of 100 × 100 m centred on each measurement station with reported macrophytes during the 2015 survey, leaving the rest of the zone free of SAV. The impact of these small patches on the overall DAV was small with the mean velocity remaining at 0.12 m/s, regardless of the parameter values used for plant densities (500, 750, or 1000 plants/m^2) and plant heights (0.35, 0.65, and 1.00 m). This was not surprising, since the relative area allocated to macrophytes remained very small, occupying only 0.76% of the study zone.

The direct comparison between measured and modelled velocity data (station by station, small patches scenario) is presented in Figure 8. The regression slope can be seen to approach unity with the modified *k*-ε model. This is probably due to the model's ability to better predict the low velocities found in the macrophyte zones. Local comparisons of velocity using only Manning's *n* showed relatively low correlations r = 0.461. When using the modified *k*-ε model the correlation increased, particularly for higher plant heights (Table 6). The modelled macrophyte height thus appears as the main driver in the increase of agreement between the measured and predicted velocities, while densification of macrophyte patches caused only minor changes. This supports the conclusion of Vargas-Luna et al. (2015) that the degree of submergence was the major factor driving flow resistance estimation. The largest correlation value (0.804 for DAV) was associated with plants (rigid cylinders) of 1.35 m. It is worth noting that, at some sampling stations, this height exceeded the total water depth, therefore resulting in a shift from fully submerged to surface floating.

3.4.2 | Comparison of vertical velocity profiles at specific stations

Velocity profiles modelled using the small-patch vegetation method (modified *k*-ε model) and the 2015 data were used to compare with

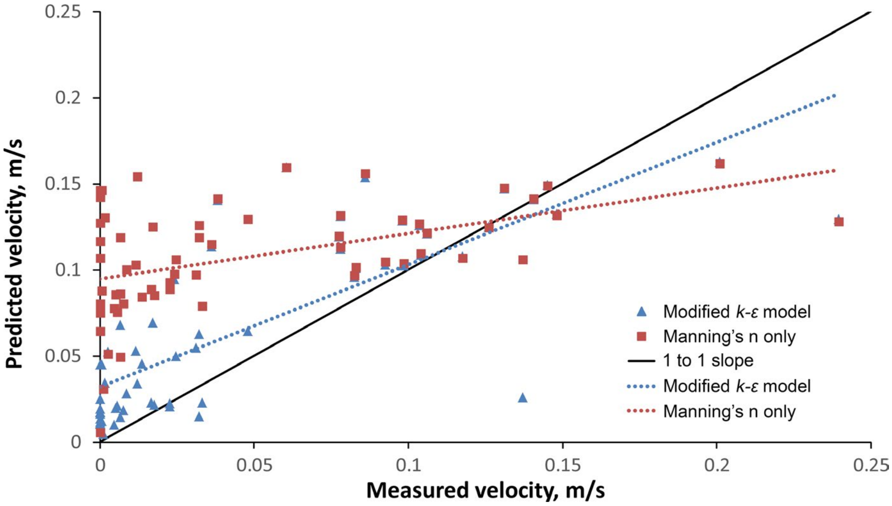

FIGURE 8 Predicted versus measured velocity for the 2015 models using Manning's *n* only (red squares) and modified *k*-ε model for depth-averaged velocity (blue triangles) [Colour figure can be viewed at wileyonlinelibrary.com]

TABLE 6 Pearson correlation (*r*) values for the comparison of modelled and measured velocities at different heights above the bottom as well as depth-averaged velocity (DAV). All comparisons are based on 62 observations for the year 2015

Model scenarios		Correlation with measured velocities in each water layer/depth averaged velocity			
Plant height, m	Plant density, plants/m^2	Bottom 0–20%	Middle 20–40%	Top 80–100%	DAV
0.35	750	0.677	0.693	0.490	0.682
0.65	500	0.690	0.771	0.633	0.744
0.65	750	0.689	0.769	0.616	0.741
0.65	1,000	0.689	0.769	0.602	0.738
1.00	750	0.695	0.785	0.742	0.790
1.00	1,000	0.695	0.784	0.739	0.789
1.35	1,000	0.699	0.789	0.783	0.804

velocities generated from the Manning's *n* only model and with field measurements. Figure 9a–d presents cases with a very good match between field velocity measurements and predicted velocities when using the modified *k*-ε model at four measurement stations. In these cases, the Manning's *n* only models (logarithmic profile) are clearly overestimating velocity. It is interesting to note that the modified *k*-ε model is able to predict well both the cases with near-zero velocity (Figure 9a,b) and with a slow, but non-zero velocity (Figure 9c,d). There are, however, also cases where neither the Manning's *n* nor the modified *k*-ε model has been able to model field observations (Figure 9e,f). For the cases where no macrophytes are reported (Figure 9g,h), the Manning's *n* only scenario results in a fairly good agreement with the measured vertical profile.

4 | DISCUSSION

This study demonstrates the successful use of a 3D hydrodynamic model to accurately assess the impact of SAV on the flow field and mean residence time in the realistic setting of a large fluvial lake. The results from this study were validated using a unique and extensive field dataset in LSP of both macrophyte density and height, as well as velocity measurements for 5 different years. The data set has allowed for the comparison of different modelling approaches that were subsequently validated with field data.

To adequately represent macrophytes in the LSP fluvial system, which if very large (47 × 13 km including the archipelago) and in particular the study zone (approximately 42 km^2), macrophytes were represented as patches instead of individual plants—a scale that currently suffers from a paucity of studies (Marjoribanks et al., 2017; Nepf, 2012). Our results are consistent with findings from previous studies, which observed a marked effect of macrophytes on the flow field (Boudreau et al., 1994; Fischer-Antze et al., 2001; Marjoribanks et al., 2014, 2017; Morin, Leclerc, et al.; 2000; Morin et al., 2003), and showed how the introduction of the modified *k*-ε model improved the accuracy of the model. It is encouraging that the relatively simple approach used in the D3D model of LSP, based on rigid cylinders, resulted in a significant flow reduction at the depths occupied by modelled macrophytes in comparison with runs where macrophytes were represented through Manning's *n* only. Velocity profiles and residence time near the riverbed predicted from the modified *k*-ε model indicated an increase in drag resulting from the presence of macrophytes. While many previous studies similarly compared velocity profiles at point locations,

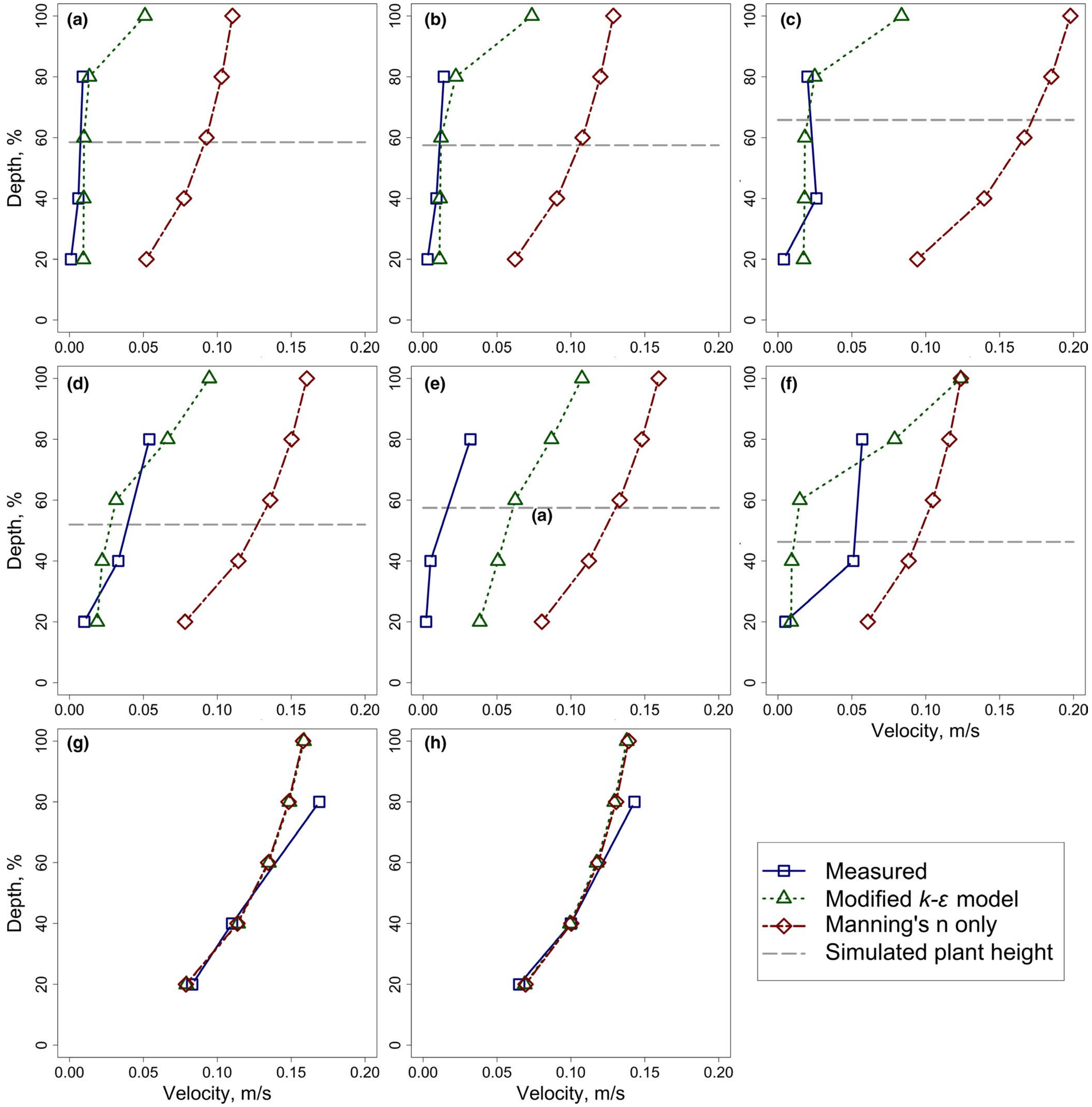

FIGURE 9 Comparison of modelled and measured velocity profiles at different measurement stations in 2015: (a–f) macrophytes present; and (g) and (h) no reported macrophytes. Based on field measurements, macrophytes were characterised having 1-m height and 750 plants/m^2 density in (a–c, e and f); 0.65 m height and 500 plants/m^2 density in D [Colour figure can be viewed at wileyonlinelibrary.com]

this was done primarily in laboratory flumes or smaller reaches (Murphy et al., 2007). The D3D LSP model successfully predicted velocities at point locations throughout the very large study zone (42 km^2).

At a reach scale, the additional resistance due to vegetation can be determined conventionally by the blockage factor (Green, 2005; Nepf, 2012; Nikora et al., 2008), which corresponds to a ratio of the cross-section occupied by a vegetation patch over the total cross section. However, such an approach is challenging to implement in a larger water body such as LSP, particularly when only a portion of the lake is studied.

Knowing the predicted variation of the flow field vertically enables an accurate estimate of residence time—a critical variable for understanding and predicting phosphorous and nitrogen transformations (Saunders and Kalff 2001; Blanton et al., 2010; Hensley, Cohen, & Korhnak, 2015). The modelled mean residence time based on DAV did not change markedly between the different tested macrophyte scenarios, reflecting the small changes in mean velocity between the runs. However, calculating mean residence time for each depth layer revealed large vertical differences in water circulation, with potential impacts on nutrient retention and absorption rates. Since biogeochemical transformations largely occur at the water–sediment interface due to strong redox gradients (Barko, Gunnison, & Carpenter, 1991; Jaynes & Carpenter, 1986; Vila-Costa et al., 2016), the presence of macrophytes is likely to increase biological retention of nutrients and contaminants through increased particle settling and the enhanced residence time of near-bottom waters. This is a main advantage of the 3D model used here, as it has the ability to predict velocities at different depths due to its use of the Navier–Stokes equations, compared to more conventionally used 2D models (based on the St Venant equations) for study zones as extensive as LSP. Indeed, results from our study could potentially help to better understand the ecological services provided by macrophytes with regards to various biogeochemical transformations, both horizontally as well as vertically in the water column.

Although the modified k-ε model produces hydraulically reasonable predictions for both low and high flow stage conditions of LSP, it is rather difficult to obtain a perfect fit between measured data and predictions at certain sampling station locations. The errors in predicting velocity could be attributed to several reasons, including the numerical mesh for the study zone, which remains fairly coarse (25 m). Marjoribanks et al. (2017) noted an improved agreement between predicted results and measured data as they increased their model mesh resolution. In our mesh resolution sensitivity tests, we concluded that the additional refinement of the study zone subdomain did not produce considerable changes in the mean velocity. Realistically, considering the scale of LSP, increasing the model mesh resolution further would have resulted in lengthy computational times or model stability issues, greatly limiting our ability to run sensitivity analysis on various macrophyte parameters. Given the scale of the study zone, the LSP model calculates a velocity value (per vertical layer) for a cell with an area of 625 m^2; thus, it is not surprising that the predicted velocity differs from the observed measurements at some measuring stations located in more dynamic zones. Furthermore, the geolocation of the field data measurements does not necessarily coincide spatially with the location of the centre of a cell value in the D3D mesh.

Another explanation for the poor predictions at some sites is that the DEM used to generate the numerical mesh has a pixel resolution of 25 m, which represents a coarse generalisation of the actual lake bed. Considering that the DEM was produced in 2002, it is likely that changes in the actual lake bathymetry have occurred due to aggradation or erosion, which has not been accounted for in the model. The confluence of SFR and SLR could be characterised as a deltaic depositional environment and there is a probability that the presence of SAV enhances further deposition. Acquiring an updated bathymetry would be valuable for future studies.

Our modelled macrophyte representation is somewhat simplified in comparison with real life conditions where there is large variability in macrophyte height and stem width both within and among different species of plants. Considering that the submerged plants are parameterised as rigid cylinders by the modified k-ε model, the modelled plants are still far from the correct depiction of the in situ aquatic plants. Since, in nature, most macrophytes are flexible and bend in the direction of the flow, the height used in the model actually represents bending height, which changes with water depth and velocity. Furthermore, in our models, vegetation patches were represented as blocks static in time, which would not react to changes in hydraulic parameters. Incorporating the ability to represent plant reconfiguration in modelling would benefit further studies on macrophyte-flow interactions by assessing the impact of flexible SAV, and thus better approximate the natural conditions in modelling (Marjoribanks et al., 2017; Verschoren et al., 2016).

Despite these drawbacks, the modelling of macrophytes in our large-scale application still produced realistic resistance to flow, where the model was able to capture near-zero velocities as measured in situ. This is a major contribution, as obtaining reliable velocity measurements in large water bodies affected by macrophytes is notoriously difficult (Ayoub et al., 2018). Considering that the D3D model is capable of approximating measured velocity magnitude, preserving the logarithmic shape throughout the water column and reaching near-zero velocities without increasing the roughness coefficient, we recommend this modelling approach for future research on the impact of macrophytes on flow at the scale of vegetation patches in large water bodies comparable to LSP.

5 | CONCLUSIONS

A 3D hydrodynamic model that represents macrophytes through a modified 3D k-ε turbulence closure model in D3D was successfully used to model the observed flow field in LSP, a large fluvial lake in the SLR system. When compared to the more traditional modelling approach using a resistance coefficient (Manning's n), predicted velocities were in better agreement with field data. Modelled residence time in an extensive zone with an area of 42 km^2 downstream from the confluence with the SFR was also longer than that predicted from the Manning's n approach, particularly close to the bed. Sensitivity analysis revealed that the additional resistance time is closely associated with plant height, and that plant density only plays a minor role. These findings indicate that it is possible to accurately quantify the impact of SAV on the flow field in large fluvial systems. Such a 3D modelling approach could be used in future studies to improve our understanding on the role of macrophytes in nutrient and pollutant dynamics for a wide range of scales.

ACKNOWLEDGMENTS

We are grateful to Stéphanie Massé, Caroline Chartier, Elena Neszvecsko, Geneviève Trottier, Magali Noiseux-Laurin, François Messier, William Massey, Joanna Gauthier, Yasmina Remnal, Jean-Pierre Amyot, Conrad Beauvais, Maude Lachapelle and Roger Gladu for their assistance in collecting field data. The comments of two anonymous reviewers are greatly appreciated. This research was funded by the Fonds de recherche de Quebec – Nature et Technologies (FRQNT) scholarships (M. Bulat, M. Botrel), Natural Sciences and Engineering Research Council of Canada (NSERC) scholarship (M. Botrel), FRQNT Strategic Initiatives for Innovation, and Natural Sciences and Engineering Research Council of Canada (NSERC) (Discovery grants P. Biron, J. Lacey, R. Maranger). This study is a contribution to the Canada-Québec St. Lawrence Action Plan.

CONFLICT OF INTEREST

The authors declare no conflict of interest.

DATA AVAILABILITY

The data that support the findings of this study are available from the corresponding author.

ORCID

Maxim Bulat https://orcid.org/0000-0002-3970-6807

REFERENCES

Aberle, J., & Järvelä, J. (2013). Flow resistance of emergent rigid and flexible floodplain vegetation. *Journal of Hydraulic Research*, *51*(1), 33–45. https://doi.org/10.1080/00221686.2012.754795

Armanini, A., Righetti, M., & Grisenti, P. (2005). Direct measurement of vegetation resistance in prototype scale. *Journal of Hydraulic Research*, *43*(5), 481–487. https://doi.org/10.1080/00221680509500146

Ayoub, F., Jones, C. E., Lamb, M. P., Holt, B., Shaw, J. B., Mohrig, D., & Wagner, W. (2018). Inferring surface currents within submerged, vegetated deltaic islands and wetlands from multi-pass airborne SAR. *Remote Sensing of Environment*, *212*, 148–160. https://doi.org/10.1016/j.rse.2018.04.035

Bal, K. D., Brion, N., Woulé-Ebongué, V., Schoelynck, J., Jooste, A., Barrón, C., … Bouma, T. J. (2013). Influence of hydraulics on the uptake of ammonium by two freshwater plants. *Freshwater Biology*, *58*(12), 2452–2463. https://doi.org/10.1111/fwb.12222

Barko, J. W., Gunnison, D., & Carpenter, S. R. (1991). Sediment interactions with submersed macrophyte growth and community dynamics. *Aquatic Botany*, *41*(1–3), 41–65. https://doi.org/10.1016/0304-3770(91)90038-7

Billen, G., Garnier, J., Ficht, A., & Cun, C. (2001). Modeling the response of water quality in the Seine River estuary to human activity in its watershed over the last 50 years. *Estuaries and Coasts*, *24*(6), 977–993. https://doi.org/10.2307/1353011

Biron, P. M., Haltigin, T. W., Hardy, R. J., & Lapointe, M. F. (2007). Assessing different methods of generating a three-dimensional numerical model mesh for a complex stream bed topography. *International Journal of Computational Fluid Dynamics*, *21*(1), 37–47. https://doi.org/10.1080/10618560701374411

Blaise, C., Gagné, F., Eullaffroy, P., & Férard, J. F. (2008). Ecotoxicity of selected pharmaceuticals of urban origin discharged to the Saint-Lawrence river (Québec, Canada): A review. *Brazilian Journal of Aquatic Science and Technology*, *10*(2), 29–51. https://doi.org/10.14210/bjast.v10n2.p29-51

Blanton, J. O., Garrett, A. J., Bollinger, J. S., Hayes, D. W., Koffman, L. D., Amft, J., & Moore, T. (2010). Transport and retention of a conservative tracer in an isolated creek–marsh system. *Estuarine, Coastal and Shelf Science*, *87*(2), 333–345. https://doi.org/10.1016/j.ecss.2010.01.010

Bolduc, P., Bertolo, A., & Pinel-Alloul, B. (2016). Does submerged aquatic vegetation shape zooplankton community structure and functional diversity? A test with a shallow fluvial lake system. *Hydrobiologia*, *778*(1), 151–165. https://doi.org/10.1007/s10750-016-2663-4

Boothroyd, R. J., Hardy, R. J., Warburton, J., & Marjoribanks, T. I. (2017). Modeling complex flow structures and drag around a submerged plant of varied posture. *Water Resources Research*, *53*, 2877–2901.https://doi.org/10.1002/2016wr020186

Boudreau, P., Leclerc, M., & Fortin, G. R. (1994). Modélisation hydrodynamique du lac Saint-Pierre, fleuve Saint-Laurent: L'influence de la végétation aquatique. *Canadian Journal of Civil Engineering*, *21*(3), 471–489. https://doi.org/10.1139/l94-051

Brito, M., Fernandes, J., & Leal, J. B. (2016). Porous media approach for RANS simulation of compound open-channel flows with submerged vegetated floodplains. *Environmental Fluid Mechanics*, *16*(6), 1247–1266. https://doi.org/10.1007/s10652-016-9481-0

Bulat, M. (2018). Three dimensional dynamics of Lake Saint-Pierre and the impact of macrophytes (Unpublished MSc thesis). Concordia University, Montreal.

Canadian Commission for UNESCO (Commission Canadienne pour l'UNESCO). (2017). Biosphere Reserves in Canada. Retrieved from http://unesco.ca/home-accueil/biosphere%20new/biosphere%20reserves%20in%20canada-%20reserves%20de%20la%20biosphere%20au%20canada

Carpenter, S. R., & Lodge, D. M. (1986). Effects of submersed macrophytes on ecosystem processes. *Aquatic Botany*, *26*, 341–370. https://doi.org/10.1016/0304-3770(86)90031-8

Cheng, N. S., & Nguyen, H. T. (2011). Hydraulic radius for evaluating resistance induced by simulated emergent vegetation in open-channel flows. *Journal of Hydraulic Engineering*, *137*(9), 995–1004. https://doi.org/10.1061/(asce)hy.1943-7900.0000377

Costa, M. B., Tavares, F. V., Martinez, C. B., Colares, I. G., & Martins, C. D. M. G. (2018). Accumulation and effects of copper on aquatic macrophytes *Potamogeton pectina*tus L.: Potential application to environmental monitoring and phytoremediation. *Ecotoxicology and Environmental Safety*, *155*, 117–124. https://doi.org/10.1016/j.ecoenv.2018.01.062

Deltares (2014). Delft3D-FLOW user manual: Delft3D - 3D/2D modelling suite for integral water solutions - Hydro-Morphodynamic. Deltares, Delft. Version 3.15.34158.

Dijkstra, J. T., & Uittenbogaard, R. E. (2010). Modeling the interaction between flow and highly flexible aquatic vegetation. *Water Resources Research*, *46*(12), W12547, https://doi.org/10.1029/2010WR009246.

Fischer-Antze, T., Stoesser, T., Bates, P., & Olsen, N. R. B. (2001). 3D numerical modelling of open-channel flow with submerged vegetation. *Journal of Hydraulic Research*, *39*(3), 303–310. https://doi.org/10.1080/00221680109499833

Garnier, J., Némery, J., Billen, G., & Théry, S. (2005). Nutrient dynamics and control of eutrophication in the Marne River system: Modelling the role of exchangeable phosphorus. *Journal of Hydrology*, *304*(1), 397–412. https://doi.org/10.1016/j.jhydrol.2004.07.040

Goyette, J. O., Bennett, E. M., Howarth, R. W., & Maranger, R. (2016). Changes in anthropogenic nitrogen and phosphorus inputs to the St. Lawrence sub-basin over 110 years and impacts on riverine export. *Global Biogeochemical Cycles*, *30*(7), 1000–1014.

Green, J. C. (2005). Modelling flow resistance in vegetated streams: Review and development of new theory. *Hydrological Processes:*

An International Journal, *19*(6), 1245–1259. https://doi.org/10.1002/(issn)1099-1085

Grenouillet, G., Pont, D., & Olivier, J. M. (2001). Linking zooplankton and juvenile fish assemblages in a large lowland river: Influence of submerged macrophytes. *Archiv für Hydrobiologie*, 383–404. https://doi.org/10.1127/archiv-hydrobiol/151/2001/383

Hensley, R. T., Cohen, M. J., & Korhnak, L. V. (2015). Hydraulic effects on nitrogen removal in a tidal spring-fed river. *Water Resources Research*, *51*(3), 1443–1456. https://doi.org/10.1002/2014wr016178

Hu, Y., Huai, W., & Han, J. (2013). Analytical solution for vertical profile of streamwise velocity in open-channel flow with submerged vegetation. *Environmental fluid mechanics*, *13*(4), 389–402. https://doi.org/10.1007/s10652-013-9267-6

Hudon, C., & Carignan, R. (2008). Cumulative impacts of hydrology and human activities on water quality in the St. Lawrence River (Lake Saint-Pierre, Quebec, Canada). *Canadian Journal of Fisheries and Aquatic Sciences*, *65*(6), 1165–1180. https://doi.org/10.1139/f08-069

Hudon, C., Cattaneo, A., Poirier, A. M. T., Brodeur, P., Dumont, P., Mailhot, Y., … de Lafontaine, Y. (2012). Oligotrophication from wetland epuration alters the riverine trophic network and carrying capacity for fish. *Aquatic sciences*, *74*(3), 495–511. https://doi.org/10.1007/s00027-011-0243-2

Janse, J. H. (1997). A model of nutrient dynamics in shallow lakes in relation to multiple stable states. *Hydrobiologia*, *342*, 1–8.

Jaynes, M. L., & Carpenter, S. R. (1986). Effects of vascular and nonvascular macrophytes on sediment redox and solute dynamics. *Ecology*, *67*(4), 875–882. https://doi.org/10.2307/1939810

Jeppesen, E., Sondergaard, E., Sondergaard, M., & Christofferson, K. (1997). *The structuring role of submerged macrophytes in lakes*. Berlin, Germany: Springer.

Julien, P. Y. (1998). *Erosion and sedimentation*. Cambridge, UK: Cambridge University Press.

Justić, D., Rabalais, N. N., & Turner, R. E. (2002). Modeling the impacts of decadal changes in riverine nutrient fluxes on coastal eutrophication near the Mississippi River Delta. *Ecological Modelling*, *152*(1), 33–46. https://doi.org/10.1016/s0304-3800(01)00472-0

Katayama, M. (2014). Stem stiffness plays a role in determining the foraging success of predators. *Hydrobiologia*, *732*(1), 173–181. https://doi.org/10.1007/s10750-014-1857-x

Kleeberg, A., Köhler, J. A. N., Sukhodolova, T., & Sukhodolov, A. (2010). Effects of aquatic macrophytes on organic matter deposition, resuspension and phosphorus entrainment in a lowland river. *Freshwater Biology*, *55*(2), 326–345. https://doi.org/10.1111/j.1365-2427.2009.02277.x

Kothyari, U. C., Hashimoto, H., & Hayashi, K. (2009). Effect of tall vegetation on sediment transport by channel flows. *Journal of Hydraulic Research*, *47*(6), 700–710. https://doi.org/10.3826/jhr.2009.3317

Kubrak, E., Kubrak, J., & Rowinski, P. M. (2008). Vertical velocity distributions through and above submerged, flexible vegetation. *Hydrological sciences journal*, *53*(4), 905–920. https://doi.org/10.1623/hysj.53.4.905

de la Chenelière, V., Brodeur, P., & Mingelbier, M. (2014). Restauration des habitats du lac Saint-Pierre: Un prérequis au rétablissement de la perchaude. *Le Naturaliste Canadien*, *138*(2), 50–61. https://doi.org/10.7202/1025070ar

Li, S. S., & Millar, R. G. (2011). A two-dimensional morphodynamic model of gravel-bed river with floodplain vegetation. *Earth Surface Processes and Landforms*, *36*(2), 190–202. https://doi.org/10.1002/esp.2033

Madsen, J. D., Chambers, P. A., James, W. F., Koch, E. W., & Westlake, D. F. (2001). The interaction between water movement, sediment dynamics and submersed macrophytes. *Hydrobiologia*, *444*(1–3), 71–84. https://doi.org/10.1023/a:1017520800568

Maine, M. A., Sune, N., Hadad, H., Sánchez, G., & Bonetto, C. (2006). Nutrient and metal removal in a constructed wetland for wastewater treatment from a metallurgic industry. *Ecological Engineering*, *26*(4), 341–347. https://doi.org/10.1016/j.ecoleng.2005.12.004

Marcogliese, D. J., Blaise, C., Cyr, D., De Lafontaine, Y., Fournier, M., Gagné, F., … Hudon, C. (2015). Effects of a major municipal effluent on the St. Lawrence River: A case study. *Ambio*, *44*(4), 257–274. https://doi.org/10.1007/s13280-014-0577-9

Marjoribanks, T. I., Hardy, R. J., Lane, S. N., & Parsons, D. R. (2014). High-resolution numerical modelling of flow-vegetation interactions. *Journal of Hydraulic Research*, *52*(6), 775–793. https://doi.org/10.1080/00221686.2014.948502

Marjoribanks, T. I., Hardy, R. J., Lane, S. N., & Tancock, M. J. (2017). Patch-scale representation of vegetation within hydraulic models. *Earth Surface Processes and Landforms*, *42*(5), 699–710. https://doi.org/10.1002/esp.4015

Martin, S., Champoux, O., & Morin, J. (2016). Modélisation des masses d'eau du fleuve Saint-Laurent au lac Saint-Pierre en support au suivi de la qualité de l'eau. Note technique NT-118, *Service météorologique du Canada, Environnement et Changement climatique Canada*, Québec. 30 pages.

Morin, J., Champoux, O., Mingelbier, M., Bechara, J. A., Secretan, Y., Jean, M., & Frenette, J. J. (2003). Emergence of new explanatory variables for 2D habitat modelling in large rivers: The St. Lawrence experience. *Canadian Water Resources Journal*, *28*(2), 249–272. https://doi.org/10.4296/cwrj2802249

Morin, J., Leclerc, M., Secretan, Y., & Boudreau, P. (2000). Integrated two-dimensional macrophytes-hydrodynamic modelling. *Journal of Hydraulic Research*, *38*(3), 163–172. https://doi.org/10.1080/00221680009498334

Murphy, E., Ghisalberti, M., & Nepf, H. (2007). Model and laboratory study of dispersion in flows with submerged vegetation. *Water Resources Research*, *43*(5).

Nepf, H. M. (2012). Hydrodynamics of vegetated channels. *Journal of Hydraulic Research*, *50*(3), 262–279. https://doi.org/10.1080/00221686.2012.696559

Nikora, N., Nikora, V., & O'Donoghue, T. (2013). Velocity profiles in vegetated open-channel flows: combined effects of multiple mechanisms. *Journal of Hydraulic Engineering*, *139*(10), 1021–1032.

Nikora, V., Larned, S., Nikora, N., Debnath, K., Cooper, G., & Reid, M. (2008). Hydraulic resistance due to aquatic vegetation in small streams: Field study. *Journal of Hydraulic Engineering*, *134*(9), 1326–1332. https://doi.org/10.1061/(asce)0733-9429(2008)134:9(1326)

O'Hare, M. T., Hutchinson, K. A., & Clarke, R. T. (2007). The drag and reconfiguration experienced by five macrophytes from a lowland river. *Aquatic Botany*, *86*(3), 253–259. https://doi.org/10.1016/j.aquabot.2006.11.004

Papanicolaou, A. N., Elhakeem, M., & Wardman, B. (2010). Calibration and verification of a 2D hydrodynamic model for simulating flow around emergent bendway weir structures. *Journal of Hydraulic Engineering*, *137*, 75-89. https://doi.org/10.1061/(asce)hy.1943-7900.0000280

Parsapour-Moghaddam, P., & Rennie, C. D. (2018). Calibration of a 3D hydrodynamic meandering river model using fully spatially distributed 3D ADCP velocity data. *Journal of Hydraulic Engineering*, *144*(4), 04018010. https://doi.org/10.1061/(asce)hy.1943-7900.0001424

Ramsar Sites Information Service. (n.d.). Retrieved from https://rsis.ramsar.org/ris/949

Rennie, M. D., & Jackson, L. J. (2005). The influence of habitat complexity on littoral invertebrate distributions: Patterns differ in shallow prairie lakes with and without fish. *Canadian Journal of Fisheries and Aquatic Sciences*, *62*(9), 2088–2099. https://doi.org/10.1139/f05-123

Sand-Jensen, K. (2003). Drag and reconfiguration of freshwater macrophytes. *Freshwater Biology*, *48*(2), 271–283. https://doi.org/10.1046/j.1365-2427.2003.00998.x

Sand-Jensen, K. (2008). Drag forces on common plant species in temperate streams: Consequences of morphology, velocity and biomass. *Hydrobiologia*, *610*(1), 307–319. https://doi.org/10.1007/s10750-008-9446-5

Saunders, D. L., & Kalff, J. (2001). Nitrogen retention in wetlands, lakes and rivers. *Hydrobiologia*, *443*(1-3), 205–212.

Schmieder, K., Werner, S., & Bauer, H. G. (2006). Submersed macrophytes as a food source for wintering waterbirds at Lake Constance. *Aquatic Botany*, *84*(3), 245–250. https://doi.org/10.1016/j.aquabot.2005.09.006

Sharpe, R. G., & James, C. S. (2006). Deposition of sediment from suspension in emergent vegetation. *Water SA*, *32*(2), 211–218.

Siniscalchi, F., & Nikora, V. (2013). Dynamic reconfiguration of aquatic plants and its interrelations with upstream turbulence and drag forces. *Journal of hydraulic research*, *51*(1), 46–55. https://doi.org/10.1080/00221686.2012.743486

Statzner, B., Lamouroux, N., Nikora, V., & Sagnes, P. (2006). The debate about drag and reconfiguration of freshwater macrophytes: Comparing results obtained by three recently discussed approaches. *Freshwater Biology*, *51*(11), 2173–2183. https://doi.org/10.1111/j.1365-2427.2006.01636.x

Talbot, A. (2006). Enjeux de la disponibilité de l'eau pour le fleuve Saint-Laurent Ŕ Synthèse environnementale. *Environnement Canada, Montréal*.

Tall, L., Caraco, N., & Maranger, R. (2011). Denitrification hot spots: Dominant role of invasive macrophyte Trapa natans in removing nitrogen from a tidal river. *Ecological Applications*, *21*(8), 3104–3114. https://doi.org/10.1890/11-0061.1

Tanino, Y., & Nepf, H. M. (2008). Laboratory investigation of mean drag in a random array of rigid, emergent cylinders. *Journal of Hydraulic Engineering*, *134*(1), 34–41. https://doi.org/10.1061/(asce)0733-9429(2008)134:1(34)

Thomaz, S. M., Dibble, E. D., Evangelista, L. R., Higuti, J., & Bini, L. M. (2008). Influence of aquatic macrophyte habitat complexity on invertebrate abundance and richness in tropical lagoons. *Freshwater biology*, *53*(2), 358–367.

Vargas-Luna, A., Crosato, A., & Uijttewaal, W. S. (2015). Effects of vegetation on flow and sediment transport: Comparative analyses and validation of predicting models. *Earth Surface Processes and Landforms*, *40*(2), 157–176. https://doi.org/10.1002/esp.3633

Verschoren, V., Meire, D., Schoelynck, J., Buis, K., Bal, K. D., Troch, P., … Temmerman, S. (2016). Resistance and reconfiguration of natural flexible submerged vegetation in hydrodynamic river modelling. *Environmental Fluid Mechanics*, *16*(1), 245–265. https://doi.org/10.1007/s10652-015-9432-1

Vila-Costa, M., Pulido, C., Chappuis, E., Calviño, A., Casamayor, E. O., & Gacia, E. (2016). Macrophyte landscape modulates lake ecosystem-level nitrogen losses through tightly coupled plant-microbe interactions. *Limnology and Oceanography*, *61*(1), 78–88. https://doi.org/10.1002/lno.10209

Vis, C., Cattaneo, A., & Hudon, C. (2008). Shift from chlorophytes to cyanobacteria in benthic macroalgae along a gradient of nitrate depletion 1. *Journal of Phycology*, *44*(1), 38–44. https://doi.org/10.1111/j.1529-8817.2007.00429.x

Wilson, C. A. M. E. (2007). Flow resistance models for flexible submerged vegetation. *Journal of Hydrology*, *342*(3), 213–222. https://doi.org/10.1016/j.jhydrol.2007.04.022

Wilson, C. A. M. E., & Horritt, M. S. (2002). Measuring the flow resistance of submerged grass. *Hydrological Processes*, *16*(13), 2589–2598. https://doi.org/10.1002/(issn)1099-1085

Wu, F. C., Shen, H. W., & Chou, Y. J. (1999). Variation of roughness coefficients for unsubmerged and submerged vegetation. *Journal of Hydraulic Engineering*, *125*(9), 934–942. https://doi.org/10.1061/(asce)0733-9429(1999)125:9(934)

Wunder, S., Lehmann, B., & Nestmann, F. (2011). Determination of the drag coefficients of emergent and just submerged willows. *International Journal of River Basin Management*, *9*(3–4), 231–236. https://doi.org/10.1080/15715124.2011.637499

Yang, W. (2008). Experimental study of turbulent open-channel flows with submerged vegetation (Doctoral dissertation, Ph. D. thesis, Yonsei University, Korea).

Yin, Y., Winkelman, J. S., & Langrehr, H. A. (2000). Long term resource monitoring program procedures: aquatic vegetation monitoring. US Geological Survey, Upper Midwest Environmental Sciences Center, La Crosse, WI. LTRMP 95-P002-7. 8 pages + appendices.

How to cite this article: Bulat M, Biron PM, Lacey JRW, Botrel M, Hudon C, Maranger R. A three-dimensional numerical model investigation of the impact of submerged macrophytes on flow dynamics in a large fluvial lake. *Freshw Biol*. 2019;64:1627–1642. https://doi.org/10.1111/fwb.13359